Controlled Synthesis of Nanoscopic Metal Cages

Jesùs Ferrando-Soria, Antonio Fernandez, Eufemio Moreno Pineda, Sarah A. Varey, Ralph W. Adams, Iñigo J. Vitorica-Yrezabal, Floriana Tuna, Grigore A. Timco, Christopher A. Muryn, and Richard E. P. Winpenny*

School of Chemistry and Photon Science Institute, The University of Manchester, Oxford Road, Manchester M13 9PL, U.K.

ⓢ *Supporting Information*

ABSTRACT: Here we show an elegant and general route to the assembly of a giant $\{M_{12}C_{24}\}$ cage from 12 palladium ions (M) and 24 heterometallic octanuclear coordination cages (C = $\{Cr_7Ni-Py_2\}$). The molecule is 8 nm in size, and the methods for its synthesis and characterization provide a basis for future developments at this scale.

Nanoscopic objects falling around 10 nm in size are difficult to make in a monodisperse form, as traditional approaches to nanoparticle synthesis tend to produce inhomogeneous materials at this size. Chemical synthesis has on rare occasions produced compounds approaching this size regime, reaching around 4 nm in diameter, for example in polyoxometalates[1,2] and in chalcogenide clusters of the coinage group metals.[3] Control of structure is difficult in these cases, and while the structures formed have in some cases been explained,[2,4] they were not fully designed in advance. Supramolecular chemistry[5] has produced many beautiful molecules but thus far has again stopped at around 4 nm.[6] This size almost seems to be a natural barrier that scientists have struggled to breach.

One of the most attractive archetypes of supramolecular chemistry is the formation of roughly spherical polyhedra with a general formula of $\{Pd_nL_{2n}\}$,[6–8] that are reminiscent of virus capsids.[9] The method offers far more control of structure than methods used to make quantum dots and nanoparticles[10,11] or template-assisted synthesis of inorganic cages.[2,4] Here we show that this methodology can be used to form far larger molecules than targeted previously while retaining complete control of complex structures. The method allows the incorporation of complex inorganic building blocks, providing a method to incorporate physical properties such as luminescence, conductivity, catalytic activity, and magnetism. This is a significant step toward tailored nanomaterials.[12]

The inorganic building block used is a chemically engineered heterometallic octanuclear coordination cage, $[^nPr_2NH_2]$- $[Cr_7Ni(\mu\text{-F})_8(O_2C^tBu)_{16}]$ (**1**),[13] hereafter abbreviated as $\{Cr_7Ni\}$. A key design feature is the very high solubility of **1** and its derivatives in noncoordinating solvents. This feature, which is easily overlooked, allows the production of very large molecules without any interference from coordinating or protic solvent and without complications caused by insolubility of side products, allowing us to make 8 nm molecules with control. These heterometallic rings have an $S = \frac{1}{2}$ ground state; as

such, they are two-level systems and are candidates as molecular qubits,[14] e.g., they have sufficient phase memory times to allow gate operations before state degradation can occur,[15] and it is also possible to control the interaction between the heterometallic rings.[16] A major question as we move toward scalable quantum devices is whether sufficient molecular qubits can be incorporated in one assembly while retaining the phase memory time; here we show that this is possible in an assembly containing 24 qubits.

We first functionalize the inorganic building block to obtain the groups needed to assemble the target nanoscopic cage (Figure 1a) and then carry out a self-assembly reaction (Figure 1b). By selective carboxylate substitution reactions on **1**,[16–18] we introduce 4′-hydroxy-4-biphenylcarboxylic acid on a Cr⋯Ni edge, giving $\{Cr_7Ni-OH\}$ (**2**) in high yield (Figure 2a). This is followed by a Steglich esterification reaction between the free alcohol functionality of **2** and 3,5-dibromobenzoic acid, leading to $\{Cr_7Ni-Br_2\}$ (**3**) (Figure 2b). The Sonogashira cross-coupling reaction of **3** and 4-ethynylpyridine hydrochloride gives the key component $\{Cr_7Ni-Py_2\}$ (**4**) (Figure 2c), which contains two widely spaced pyridine groups attached to an inorganic nanocluster in a predefined geometry. **2**, **3**, and **4** have been fully characterized by single-crystal X-ray crystallography (Figure 2 and Table S1 in the Supporting Information (SI)), elemental analysis, and mass spectrometry (full experimental details are given in the SI).

To assemble the 8 nm cage, we react **4** with $Pd(BF_4)_2 \cdot 4CH_3CN$ (2:1 molar ratio) in acetone at 50 °C over 12 h, which produces $\{Pd_{12}\{Cr_7Ni-Py_2\}_{24}\}$ (**5**) (Figure 1b). The bulk material gives a full elemental analysis consistent with this formulation, but further characterization of a compound as large as **5** is a major challenge. We have developed a method based on a suite of characterization techniques. Crystals of **5** form but do not diffract X-rays well; this is probably because **5** forms 8 nm spheres with a largely hydrocarbon exterior, and therefore, while the spheres can pack efficiently, there are no intermolecular interactions to require individual molecules to adopt the same orientation as their neighbors. This problem is similar to that faced with early structural studies of C_{60}, albeit in a molecule two orders of magnitude bigger.

Atomic force microscopy (AFM) of a drop-cast acetone solution of **5** onto a highly ordered pyrolytic graphite (HOPG) substrate (Figures 3 and S5) strongly supports the formation of an array of 8.2 ± 0.2 nm sized particles with a uniform height
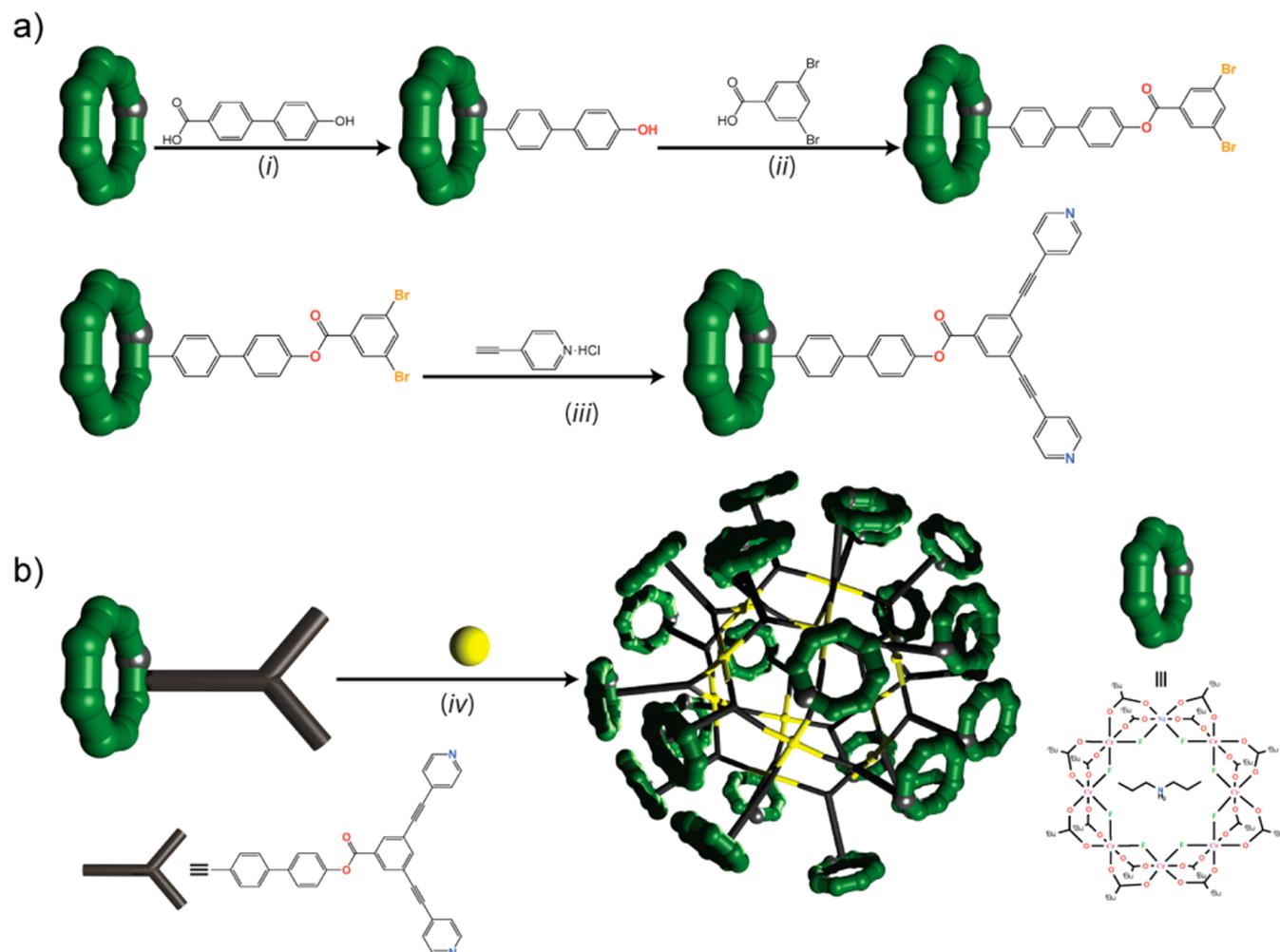
Figure 1. (a) Synthesis of key component {Cr$_7$Ni-Py$_2$} (**4**): (*i*) toluene, 1,2-dichlorobenzene, and dimethylformamide with stirring at 150 °C for 12 h; (*ii*) dicyclohexylcarbodiimide and 4-(dimethylamino)pyridine in dry THF with stirring at room temperature for 48 h under argon; (*iii*) copper(I) iodide, bis(benzonitrile)palladium(II) dichloride, diisopropylamine, and tri-*tert*-butylphosphine in 1,4-dioxane with stirring at 50 °C for 20 h under argon. (b) Self-assembly of the supramolecular inorganic cage of cages: (*iv*) Pd(BF$_4$)$_2$ ·4CH$_3$CN in acetone with stirring at 50 °C for 12 h.
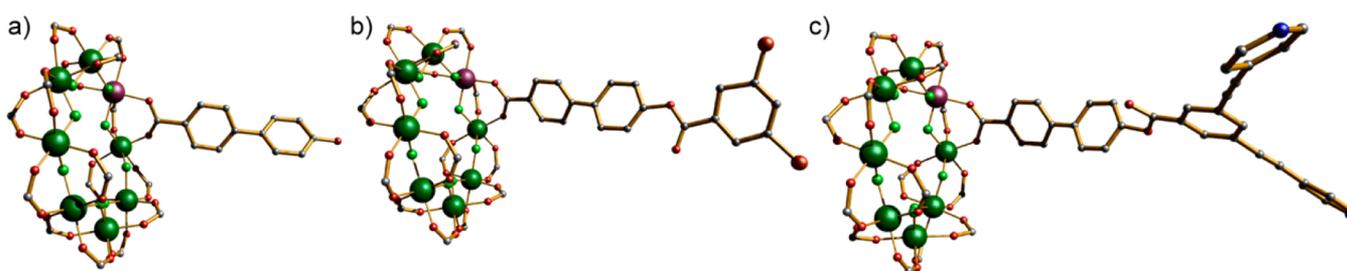

Figure 2. Single-crystal X-ray structures of (a) **2**, (b) **3**, and (c) **4**. Color code: Cr, green; Ni, purple; N, blue; O, red; C, gray; F, pale green; Br, orange. ^{n}Pr$_2$NH$_2$, H atoms, and *tert*-butyl groups have been omitted for clarity.

consistent with the expected diameter for the desired compound; the complex is stable under AFM conditions. Under the same experimental conditions, a control AFM experiment on the known {M$_{12}$L$_{24}$} polyhedron **6**, which is the core of **5** (L = 2,6-bis(pyridin-4-ylethynyl)pyridine),[19] showed an array of 4.3 ± 0.3 nm sized particles (Figure S6), which agrees with the X-ray crystal structure for this sphere (4.5 ± 0.5 nm).

To characterize the elemental composition of the film of **5** used for AFM, we performed scanning electron microscopy–energy-dispersive X-ray spectroscopy (SEM-EDX), which

revealed the presence of Cr(III), Ni(II), and Pd(II) metal ions in a homogeneous spatial distribution (Figure S7). Furthermore, in order to quantify the presence of these elements, X-ray photoelectron spectroscopy (XPS) was carried out and yielded the expected ratios between the metal ions constituting the inorganic cage (ratio calcd, ratio found for {Pd$_{12}${Cr$_7$Ni-Py$_2$}$_{24}$}: Cr/Ni (7.00, 6.85), Ni/Pd (2, 2.08), Figure S8). This remarkable agreement supports the formation of complete molecules of **5** rather than incomplete palladium cages bridged by **4**. The material therefore appears to be monodisperse.
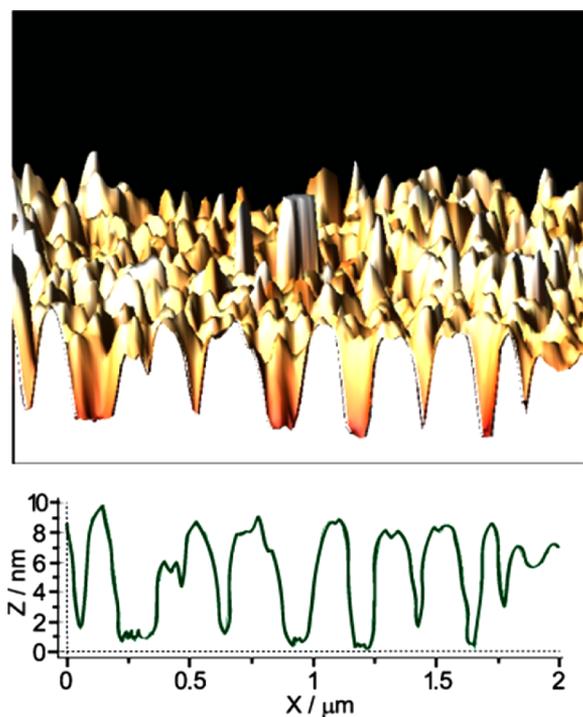
Figure 3. Physical characterization of **5**: (top) 3D AFM image; (bottom) AFM height profile.

Diffusion-ordered NMR spectroscopy (DOSY) is a powerful tool to estimate the size of roughly spherical species.[20,21] To allow DOSY to be used here, we exploited the chemical versatility of the heterometallic rings and synthesized the Co(II) version of these systems (see the SI), which are known to give interpretable NMR spectra.[22] The ^{1}H NMR spectrum of $\{Cr_7Co-Py_2\}$ (**4b**) showed the characteristics of a paramagnetic heterometallic ring (Figure S9). The ^{1}H NMR spectrum of $\{Pd_{12}\{Cr_7Co-Py_2\}_{24}\}$ (**5b**) (Figure S10) exhibited signals broader than those for **4b**. Although some of the signals in the DOSY spectra are strongly influenced by the paramagnetic centers and overlap with the solvent signals, measurement of diffusion coefficients was performed (Figures S11 and S12). A simple comparison of the diffusion coefficient (D) values for **4b** and **5b** ($D_{4b} > D_{5b}$) shows that a very large entity has been assembled. The DOSY spectrum of **5b** gives the diffusion coefficient $D_{5b} = 0.911 \times 10^{-10}$ m^2 s^{-1}, from which the Stokes–Einstein equation gives a diameter of 9.4 nm.

The proposed structure of **5** is further confirmed by solution-phase small-angle X-ray scattering (SAXS) (Figure 4).[23] We performed SAXS on concentrated solutions of **6** in dimethyl sulfoxide (Figure S13). The experimental SAXS electron density pair distribution functions obtained for **6** with broad maxima at 4.0 nm matched perfectly with the distances obtained by X-ray crystallography.[19] Concentrated solutions of **4** and **5** in tetrahydrofuran were measured. SAXS measurements on **4** (Figure S14) give the X-ray scattering for a single ring and hence allow the assignment of the maxima corresponding to the heterometallic ring in the spectra of **5**.

The first noticeable feature in **5** was a significant change in the X-ray scattering compared with **4** and **6**. The analysis of the diffraction data with a pair distance distribution function shows pairs of particles separated by much larger distances, with the maximum extent being ca. 8.0 nm. The model is therefore consistent with 24 $\{Cr_7Ni-Py_2\}$ rings about a central supramolecular platform of 12 palladium ions and matches the proposed structure of **5** (Figure 1b). The combination of AFM, SEM-EDX, XPS, ^{1}H NMR, and SAXS data allows us to predict the overall structure of **5** with confidence. It is again the very high solubility that enables this to work, allowing a suite of solution techniques and also surface techniques as we can drop-cast films. Unfortunately, electrospray ionization mass spectrometry was unsuccessful, as we could not find conditions under which these massive molecules remained intact in the gas phase. High-resolution transmission electron microscopy was indecisive, as the sample decomposed rapidly in the electron beam.

One possible use of such a molecular assembly is as a route to scalable devices based on molecular qubits, where a key factor is the phase memory time.[15,24] To measure the phase memory times, we performed pulsed electron paramagnetic resonance (EPR) spectroscopy on **4** and **5** (Figure S15–S18). The results are extremely promising, especially as no attempt was made to optimize the system for phase memory. For compound **4** we found a phase memory time of 410 ns, which is in the normal range for $\{Cr_7Ni\}$ rings.[15] For **5**, where we have brought together 24 spin centers in a molecular ensemble, we found a phase memory time of 350 ns. The estimated spin···spin distances in **5** fall in the range of 3.2 nm, and clearly this does not introduce significant decoherence effects. Magnetic susceptibility measurements showed temperature-dependent behavior for a single ring, indicating that ring···ring interactions are weak (Figure S19).

The principles employed here are broadly applicable to make further massive molecules. We are targeting still larger assemblies by using hybrid inorganic–organic rotaxanes[22] and assemblies where the molecular qubits have longer inherent phase memory times,[24] which could allow spin manipulation experiments in nanomaterials containing 24 or more electron spins. As the design of the synthetic method is modular, many other physical properties could be included. For example, luminescent or redox-active groups could be easily included.

■ ASSOCIATED CONTENT

Ⓢ Supporting Information

Preparation and physical characterization data (Figures S1–S19 and Tables S2 and S3) and crystallographic refinement details for **2**–**4** (Table S1). The Supporting Information is available free of charge on the ACS Publications website at DOI: 10.1021/jacs.5b04664. Crystallographic data were deposited at the Cambridge Crystallographic Data Centre as CCDC-1052348 (**2**), CCDC-1052349 (**3**), and CCDC-1052350 (**4**).
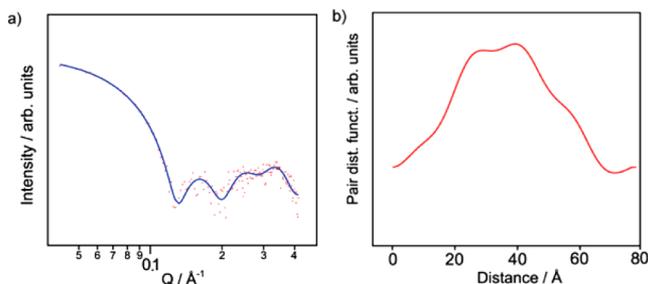

Figure 4. (a) Experimental SAXS data for compound **5**. The solid line is the fit associated with the pair distribution function plot shown in (b).

■ AUTHOR INFORMATION

Corresponding Author

*richard.winpenny@manchester.ac.uk

Notes

The authors declare no competing financial interest.

■ ACKNOWLEDGMENTS

■ REFERENCES

(1) Müller, A.; Beckmann, E.; Bögge, H.; Schmidtmann, M.; Dress, A. *Angew. Chem., Int. Ed.* **2002**, *41*, 1162.

(2) Miras, H. N.; Cooper, G. J. T.; Long, D.-L.; Bögge, H.; Müller, A.; Streb, C.; Cronin, L. *Science* **2010**, *327*, 72.

(3) Fuhr, O.; Dehnen, S.; Fenske, D. *Chem. Soc. Rev.* **2012**, *42*, 1871.

(4) Müller, A. *Nat. Chem.* **2009**, *1*, 13.

(5) Lehn, J.-M. *Supramolecular Chemistry: Concepts and Perspectives*; Wiley-VCH: Weinheim, Germany, 1995.

(6) (a) Stang, P. J.; Olenyuk, B. *Acc. Chem. Res.* **1997**, *30*, 502. (b) Leininger, S.; Olenyuk, B.; Stang, P. J. *Chem. Rev.* **2000**, *100*, 853. (c) Seidel, S. R.; Stang, P. J. *Acc. Chem. Res.* **2002**, *35*, 972. (d) Fujita, M.; Tominaga, M.; Hori, A.; Therrien, B. *Acc. Chem. Res.* **2005**, *38*, 371. (e) Gosh, S.; Mukherjee, P. S. *J. Org. Chem.* **2006**, *71*, 8412. (f) Pluth, M. D.; Bergman, R. G.; Raymond, K. N. *Acc. Chem. Res.* **2009**, *42*, 1650. (g) Chakrabarty, R.; Mukherjee, P. S.; Stang, P. J. *Chem. Rev.* **2011**, *111*, 6810. (h) Ward, M. D.; Raithby, P. R. *Chem. Soc. Rev.* **2013**, *42*, 1619. (i) Ronson, T. K.; Zarra, S.; Black, S. P.; Nitschke, J. R. *Chem. Commun.* **2013**, *49*, 2476.

(7) Tominaga, M.; Suzuki, K.; Kawano, M.; Kusukawa, T.; Ozeki, T.; Sakamoto, S.; Yamaguchi, K.; Fujita, M. *Angew. Chem., Int. Ed.* **2004**, *43*, 5621.

(8) Sun, Q.-F.; Iwasa, J.; Ogawa, D.; Ishido, Y.; Sato, S.; Ozeki, T.; Sei, Y.; Yamaguchi, K.; Fujita, M. *Science* **2010**, *328*, 1144.

(9) Lucas, W. *Viral Capsids and Envelopes: Structure and Function*; Wiley-VCH: Weinheim, Germany, 2010.

(10) Son, D. I.; Kwon, B. W.; Park, D. H.; Seo, W.-S.; Yi, Y.; Angadi, B.; Lee, C.-L.; Choi, W. K. *Nat. Nanotechnol.* **2012**, *7*, 465.

(11) Mocatta, D.; Cohen, G.; Schattner, J.; Millo, O.; Rabani, E.; Banin, U. *Science* **2011**, *332*, 77.

(12) Sanchez, C.; Shea, K. J.; Kitagawa, S. *Chem. Soc. Rev.* **2011**, *40*, 471.

(13) Larsen, F. K.; McInnes, E. J. L.; El Mkami, H.; Overgaard, J.; Piligkos, S.; Rajaraman, G.; Rentschler, E.; Smith, A. A.; Smith, G. M.; Boote, V.; Jennings, M.; Timco, G. A.; Winpenny, R. E. P. *Angew. Chem., Int. Ed.* **2003**, *42*, 101.

(14) Troiani, F.; Ghirri, A.; Affronte, M.; Carretta, S.; Santini, P.; Amoretti, G.; Piligkos, S.; Timco, G.; Winpenny, R. E. P. *Phys. Rev. Lett.* **2005**, *94*, 207208.

(15) Wedge, C. J.; Timco, G. A.; Spielberg, E. T.; George, R. E.; Tuna, F.; Rigby, S.; McInnes, E. J. L.; Winpenny, R. E. P.; Blundell, S. J.; Ardavan, A. *Phys. Rev. Lett.* **2012**, *108*, 107204.

(16) Timco, G. A.; Carretta, S.; Troiani, F.; Tuna, F.; Pritchard, R. J.; Muryn, C. A.; McInnes, E. J. L.; Ghirri, A.; Candini, A.; Santini, P.; Amoretti, G.; Affronte, M.; Winpenny, R. E. P. *Nat. Nanotechnol.* **2008**, *4*, 173.

(17) Whitehead, G. F. S.; Moro, F.; Timco, G. A.; Wernsdorfer, W.; Teat, S. J.; Winpenny, R. E. P. *Angew. Chem., Int. Ed.* **2013**, *52*, 9932.

(18) Whitehead, G. F. S.; Ferrando-Soria, J.; Christie, L. G.; Chilton, N. F.; Timco, G. A.; Moro, F.; Winpenny, R. E. P. *Chem. Sci.* **2014**, *5*, 235.

(19) Harris, K.; Sun, Q.-F.; Sato, S.; Fujita, M. *J. Am. Chem. Soc.* **2013**, *135*, 12497.

(20) Avram, L.; Cohen, Y. *Chem. Soc. Rev.* **2015**, *44*, 586.

(21) Pelta, M. D.; Morris, G. A.; Stchedroff, M. J.; Hammond, S. J. *Magn. Reson. Chem.* **2002**, *40*, S147.

(22) Lee, C.-F.; Leigh, D. A.; Pritchard, R. G.; Schultz, D.; Teat, S. J.; Timco, G. A.; Winpenny, R. E. P. *Nature* **2009**, *458*, 314.

(23) O'Sullivan, M. C.; Sprafke, J. K.; Kondratuk, D. V.; Rinfray, C.; Claridge, T. D. W.; Saywell, A.; Blunt, M. O.; O'Shea, J. N.; Beton, P. H.; Malfois, M.; Anderson, H. L. *Nature* **2011**, *469*, 72.

(24) Bader, K.; Dengler, D.; Lenz, S.; Endeward, B.; Jiang, S.-D.; Neugebauer, P.; van Slageren, J. *Nat. Commun.* **2014**, *5*, No. 5304.